Substrate-guided wave optical true-time delay feeding network for phased-array antenna steering

Bing Li, Yihong Chen, Zhenhai Fu, and Ray T. Chen
University of Texas at Austin, PRC/MER 1.606, Austin, TX 78758

Suning Tang
Radiant Research Inc.

ABSTRACT

An optical realization of the Blass matrix based on a substrate-guided wave true-time delay (TTD) module has been proposed and designed for a photonic phased-array antenna (PAA) system, which will operate from 18 to 26GHz. It is the highest RF frequency range for system level that has been reported until now. A 3×8 triangular array lattice will be used and all the elements divided into 8 sub-arrays controlled optically by true-time delay signal. To avoid the squint error caused by the phase control within the subarray, we propose a new squint-free subarray steering technique, which is based on the operation of the true-time delay signals provided by our new optical TTD Blass matrix. The simulation result is given for the far-field radiation pattern of photonic PAA controlled by this technique and no squint is found. We also demonstrate an optical heterodyne system for photonic RF signals generation with conversion efficiency that approaches the theoretical limit.

Keywords: Optical true-time delay, photonic signal processing, phased-array antenna, optical interconnect.

1. INTRODUCTION

Significant effort has been applied to photonic phased-array antenna techniques, in which the radiation steering of an array antenna is accomplished by optical true-time delay control. It is expected that a compact and practical true-time delay beamforming network based on photonic signal processing techniques can be realized. Upon that, we can provide the feeding signals for the array elements with correct phase relationship at any RF frequency; in other words, we can avoid the beam squint that is the main drawback of conventional phased-array antenna based on phase-shift control designed at a single RF frequency. Owing to the advantages of the photonic signal processing technique, several promising techniques for optical TTD have been presented as well as the system demonstration for photonic PAA [1-8]. One of the most important structures for optical TTD is the delay path selection controlled by the integrated optical waveguide switch. The long scale delay path will be made by optical fibers, the short scale path directly integrated with the switch on one photonic channel waveguide chip[6]. A good example of such a structure is the binary fiber optic delay line (BIFODEL)[4]. The problem with BIFODEL or other delay path selection techniques by electro-optical switch is insertion loss and crosstalk, due to the limited performance of optical waveguide switches and the cascaded structure. In theory, similar structures such as 4×4 or 8×8 switch matrices[5] can reduce the levels of cascade and so the insertion loss and crosstalk, but they are impractical because the practical multi-port crossbar switch itself consists of a binary switch matrix.

In our previous work, we demonstrated the compact optical true-time delay module based on substrate-guided wave structure[9]. It is a broadcast (fanout) structure and the delay signal taping is accomplished by the holographic volume grating that was recorded on the top surface of the glass substrate. Using uniform grating, a 2-D optical fanout of the delayed signal can be formed and the delay step is limited by the thickness of the substrate and ultimately the diameter of the optical beam spot. This old design is not suitable for phased-array antennas operating at high RF frequency range. For example, the K-band array antenna that operates from 18-26GHz will require sub-picosecond delay control for just 5-bit steering resolution. So a new scheme of an optical true-time delay feeding network has to be used to control the steering of high RF frequency phased-array antennas.

In this paper, we propose an optical realization of the Blass matrix for true-time delay steered array-antennas, a proposal that is based on our substrate-guided wave/hologram grating fanout structure. We have under preparation a K-band photonic phased-array antenna system demonstration using this novel design. Here we report our system configuration, array lattice

structure, and the simulation result of a far-field radiation pattern. In most system experiments, the entire aperture of the antenna was routinely divided into a series of subarrays and based upon that, the true-time delay control was applied. With this method, the scale of the whole system can be reduced, although a little squint still occurs because the phase-shift steering must be used within each subarray. To overcome this problem in our system demonstration, we propose a new steering technique for the subarray and we demonstrate in theory the squint-free property. Finally, we also report a two-lasers heterodyne experiment, which is for the photonic RF signal generation with the conversion efficiency at its theoretical limit.

2. BEAMFORMING MATRIX FOR TRUE-TIME DELAY STEERING OF ANTENNA

Assuming that the direction gain of the array elements is uniform, the radiation pattern of a linear array with *K* elements will be:

$$R(\theta) = \sum_{k=0}^{K-1} A_k \exp(-j \cdot 2\pi f k \cdot \tau) \cdot \exp(j \cdot 2\pi k \cdot \nu \cdot \sin\theta) \tag{1}$$

where θ is the radiation angle referring to the normal direction of antenna aperture; ν = D / λ, the ratio between the array lattice period and the radiation wavelength; and τ is the time-delay between the neighboring array elements. Thus, for a certain steering angle θ_c , the required τ is:

$$\tau = \frac{D}{\lambda f} \cdot \sin\theta_c = D \cdot \sin\theta_c / c \tag{2}$$

It is obvious that $\Delta\tau$ depends only on the array lattice parameters and the steering angle, and is unrelated to the radiation frequency. That is the reason why the true-time delay controlled PAA is able to operate for wide-band application. On the contrary, if one uses the phase-shift steering, the control variable $\psi = f \cdot \tau$ has to be designed under certain radiation frequencies, and squint occurs when the frequency changes.

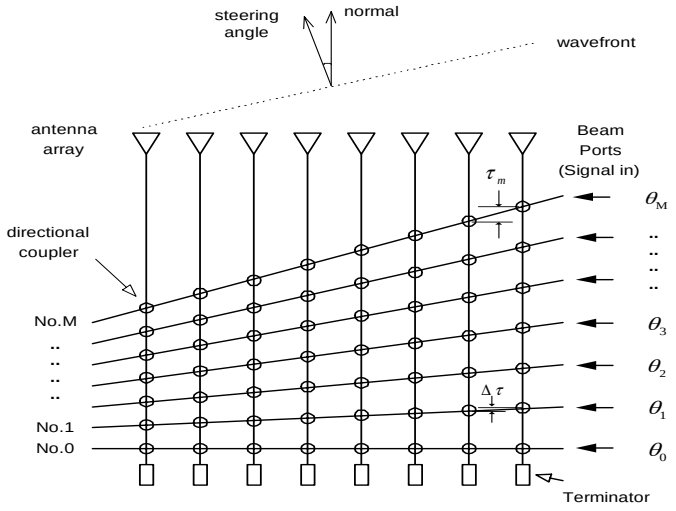

Fig.1 Beamforming matrix (Blass) of phased-array antenna

The above true-time delay steering can be realized by the beamforming matrix, also called the Blass matrix [10], as shown in Fig.1. When the signal is fed into one of the series of input lines, it is distributed to all the elements through the directional coupler nodes along the line. And the time delay between the neighboring elements is determined by the length difference of the transmission lines from the nodes to the corresponding elements plus the increment of the propagation distance between the nodes. One should notice that a delay corresponding to the horizontal distance between the neighbor nodes has to be compensated before the radiation, in order to get the zero steering angle by feeding the signal from the input line on the horizontal direction. Through designing the tilt angle of all these input lines, from No.*0* to No. *M*, we can let the delay time τ increase by the step of $\Delta\tau$, which will be required by the steering angle resolution according to this formula,

$$\tau_m = m \cdot \Delta\tau = m \cdot \Delta U \cdot D / c \tag{3}$$

where ΔU is the steering angle resolution that is defined as:

$$\Delta U = (\sin\theta_{MAX}) / M \tag{4}$$

and M is the number of steering angle positions. Then, for the minus angle steering, all we need to do is simply reverse the tilt direction of the input lines.

3. OPTICAL TRUE-TIME DELAY BEAMFORMING MATRIX

For an electrical antenna, the Blass matrix above is only a theoretical scheme. It is impractical to try to build this kind of matrix by microwave transmission line or waveguide. However, our substrate-guided wave optical true-time delay technique gives a real opportunity to realize it the optical domain. The idea is, instead of directly using the delay introduced by one step bouncing as $\Delta\tau$, we can make a series of bouncing paths within the guiding-wave substrate with different steps that actually become an increasing sequence. Then, we bring $\Delta\tau$ to the neighboring antenna elements by the difference between the time-step of the neighboring bouncing path and the accumulation of this difference. The resulting optical true-time delay module will have the structure as shown in Fig.2.

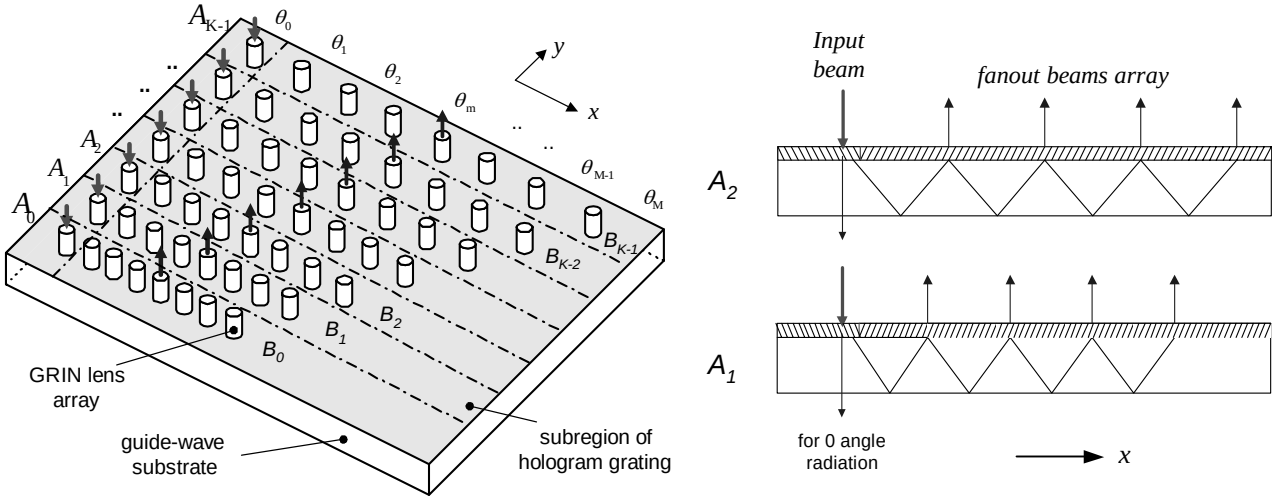

Fig.2 Optical Blass matrix based on guide-wave substrate

The module is built on the guiding-wave substrate with a thickness of h. On the top-surface of the substrate, there is a transparent grating film made by the hologram recording. The whole grating surface was divided into several sub-regions (Fig.2). The grating is uniform within each sub-region,, but not among them. As shown, the A_k series is the input grating group, and the B_k series is the output group. Each pair (A_k, B_k) has the same value of diffraction angle α_k but a reverse tilt direction. Actually, index k here merely corresponds to the array element number of the antenna. Through input grating A_k, the K channels of light (optical RF signal) can be coupled into the substrate with angles larger than the criteria of complete reflection. So a zigzagging propagation will happen along x. At each bouncing step, the output grating extracts part of the light from the substrate again and generates a normal fanout beam. As a result, a 2-D fanout array, which is a matrix with K-rows and M-columns, will be formed all over the surface of the guiding-wave substrate. The diffraction angle of grating α_k increases gradually with index k. The desired α_k sequence should be able to let the 2-D fanout array become linearly non-uniform, which means that the bouncing step's length should increase linearly along k. Assuming the K channels of light have the exactly same time-phase when they arrive the input ports $\{A_k\}$, the introduced time delay by the module between fanout (k, m) and (k+1, m) is:

$$\tau_m = m \cdot \Delta\tau = m \cdot \frac{2nh}{c}\left[\frac{1}{\cos(\alpha_{k+1})} - \frac{1}{\cos(\alpha_k)}\right] \tag{5}$$

Then substitute $\Delta\tau$ required by (3) and (4) into (5), the required diffraction angle sequence $\{\alpha_k\}$ can be calculated. In next section, we will give a design instance for our system demonstration.

Another issue is the diffraction efficiency. For the input grating group, diffraction efficiency η_A shall not be 100%, but quite close. The transmitted part will be the control signal for normal radiation of the array antenna. For the output grating B_k, the efficiency shall be the function $\eta_B^k(x)$, designed according to the bit-number of steering. In order for the fanout beam array to have a uniform power distribution along *x*, the corresponding efficiency series must satisfy,

$$\eta_B^k(x_m) = \eta_B^k(x_{m-1}) / [1 - \eta_B^k(x_{m-1})] \tag{6}$$

where x_m is the location of the fanout point on the *x*-axis. For instance, with 3-bit steering resolution and assuming that the largest efficiency is η_{Maz} = 90%, the resulting efficiency series $\{\eta_B^k(x_m)\}$ will be 12.3%, 14%, 16.3%, 19.5%, 24.2%, 32%, 47%, 90%. The insertion loss will be 9.1dB.

In this optical ture-time delay Blass matrix, the substrate functions as the waveguide-array that brings signal to the antenna array in Fig.1 The hologram grating works as the directional coupler array. Different from Fig.1, we use the post-switching method to select the output delayed signal series (columns of the matrix) instead of using pre-switching to select the input port series. The fanout beams will directly illuminate the wide-band photodetectors through a GRIN lens to accomplish the O/E conversion. Then, the signals selection and switching can be excuted in electrical domain. Another, simpler way would be simply to combine the RF output of all the photodetectors on the same row of the matrix, then switch the desired photodetector ON and the others OFF [10] to select, as discussed in detail below. The fanout beam series corresponding to the different steering angles are shown in in Fig.2.

Here we notice that the size of the structure shown in Fig.2 increases rapidly with the total elements number *K* of the antenna and the bit-number $\log_2 M$ of angle steering. For large *K*, the solution is to interrupt the increase of diffraction angle α_k, and use multi-bouncing as one step instead of single-bouncing. For large *M*, we use a multi-level cascaded scheme, instead of a single module, to produce all the delay signals: first, divide the whole steering angle range into several sub-ranges, two sub-ranges, for example. Then we use one module, with a large enough delay step to accomplish the first level steering. That way, the delay relationship among *K* channels of light shall be able to steer the antenna to the beginning angle of the desired sub-range. Finally, we use another module with a small delay step to finish the fine steering within the sub-range. Another level can be added to this scheme with the wavelength shift, in order to provide the tiny resolution on angle steering [11].

4. STEERING FEEDING NETWORK AND PAA SYSTEM DESIGN

The optical true-time delay feeding network for phased-array antenna steering based on above optical Blass matrix and the antenna system configuration are shown in Fig.3.

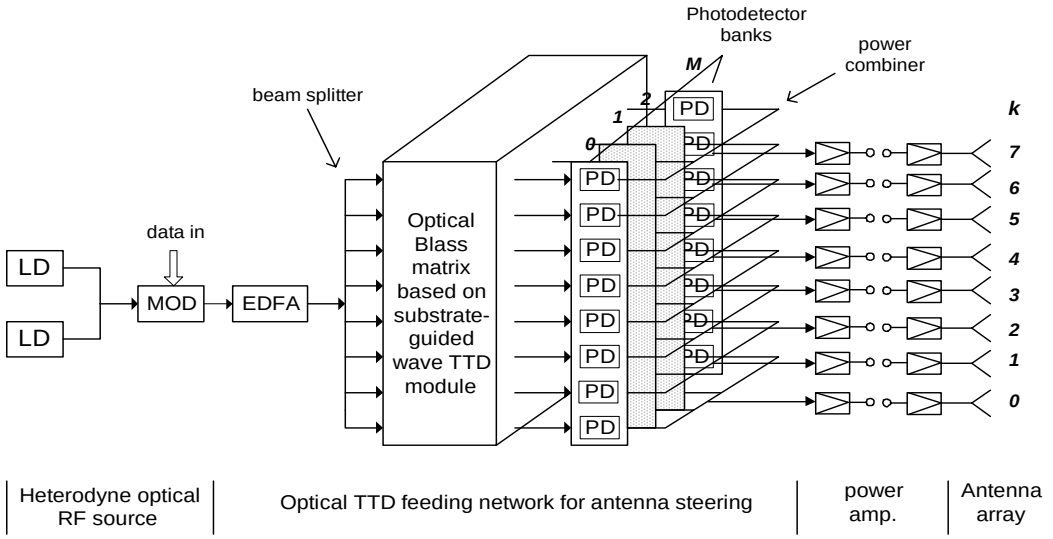

Fig.3 Optical TTD feeding network and photonic phased-array antenna system configuration

The design target of this photonic phased-array antenna system is to provide the instantaneous RF bandwidth of 18-26GHz, angle resolution 3-bit at the steering range of 0 ~ 45 deg., and the normal beamwidth less than 9 deg. An optical heterodyne system can be used to generate the photonic RF signal with tunable frequency range up to 30 GHz. The EDFA boosts the optical power up and the beam splitter divides the light into $K = 8$ channels, which correspond to the number of subarrays of the antenna. After the optical Blass matrix, M+1 columns of fanout beams will be produced corresponding to the M+1 steering angles (including normal radiation). In this system, we prepare to demonstrate 3-bit angle steering, so $M = 8$. Each column of optical fanout will be converted to K-channels RF signal by a wide-band photodetector bank. There is a total of M+1 photodetector banks, and each bank has K=8 photodetectors. The outputs of the photodetectors that have the same sequent number (k) will be combined together with the same electrical length. So, finally, K=8 channels of RF signal are fed into the input-ports of antenna. Of course, a power amplifier stage will always be needed before the final radiation.

If all the photodetectors operate in the ON state, the antenna will have multi-beams. Specifically, there are M+1=9 radiation beams out of the antenna array with different angles. If we turn on only one bank of the photodetectors and turn off the others, only one radiation beam will correspondingly exist. When we switch the photodetector banks ON/OFF alternatively, the antenna can then be steered. With this method, the delay signal selection and O/E conversion can be finished within one stage and so the system complexity can be reduced. The switching of the wide-band photodetector will be accomplished by controlling its bias voltage. The characteristics of this operation have been reported elsewhere [12].

The 24 elements of phased-array antenna will be provided by Atlantic Aerospace Electronics Corp. It has a lattice structure (shown in Fig.4). A 45º triangular lattice is used to expand the elements' interval and depress the grating lobe at the same time. The whole aperture will be divided into 8 sub-arrays. Each sub-array has the combination {k, k+8, k+16}.

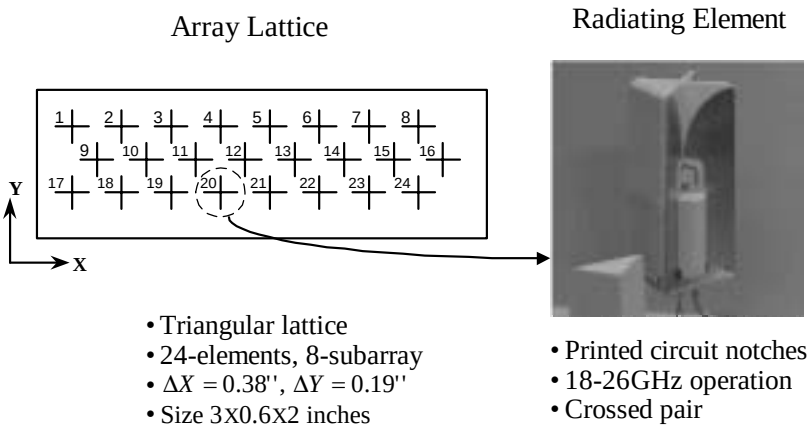

Fig.4 Antenna array lattice and radiation element structure

In our experiment, this 3-row array antenna works as a linear array, which means that we only provide the TTD control for steering in X-Z plane. In that case, the first and third row will use the same signal, and the middle row will require a phase deviation from them. The interval distance between neighboring subarrays is ΔX=0.38", or 9.652mm. The designed steering angle range is 0 ~ 45°. We use the substrate with a thickness of 3 mm to build the optical TTD module, for 3-bit resolution, the designed diffraction angle series according formulas (3), (4), and (5) as given in Table 1:

Table.1 Diffraction angle α_k, fanout interval T_k, and bouncing step length L_k.

α_k (deg.)	T_k (mm)	L_k (mm)
42	5.402424	8.073796
46.0312	6.219939	8.642201
59.3510	6.988223	9.210605
52.1527	7.721985	9.77901
54.5597	8.430243	10.347415
56.6562	9.118943	10.91582
58.5029	9.792212	11.484224
60.1443	10.453032	12.052629

The resulting delay step $\Delta\tau$ is 2.8457 ps. It corresponds to the difference 0.5684 mm between L_k and L_{k+1}.

The 8-channels true-time delay signal provided by the optical steering feeding network will be used to control the 8 subarrays. Within each subarray, the element *m* in the first row will get the direct copy of the input TTD signal. So, the first row is a true time-delay controlled row. The third row will be discarded because, according to our simulation, it increases the grating lobe problem. For the middle row, the typical method is to use the phase-delay control as in the conventional PAA system. The phase deviations for steering will be designed on 22GHz, that is, the center frequency of the radiation bandwidth. In that case, the steering of the antenna is actually controlled by a hybrid scheme: true-time delay among subarrays and phase-delay within the subarray. Fig. 5 shows the simulation result on the far-field radiation pattern of the antenna under this hybrid control scheme. A small squint error appears as we can see from the pattern at 45 degree steering angle. Even though we have to zoom in the pattern to see this small squint, it is still a big issue for wide-band phased-array antenna. In our discussion below, we introduce a new subarray control technique to eliminate this small (but important) error.

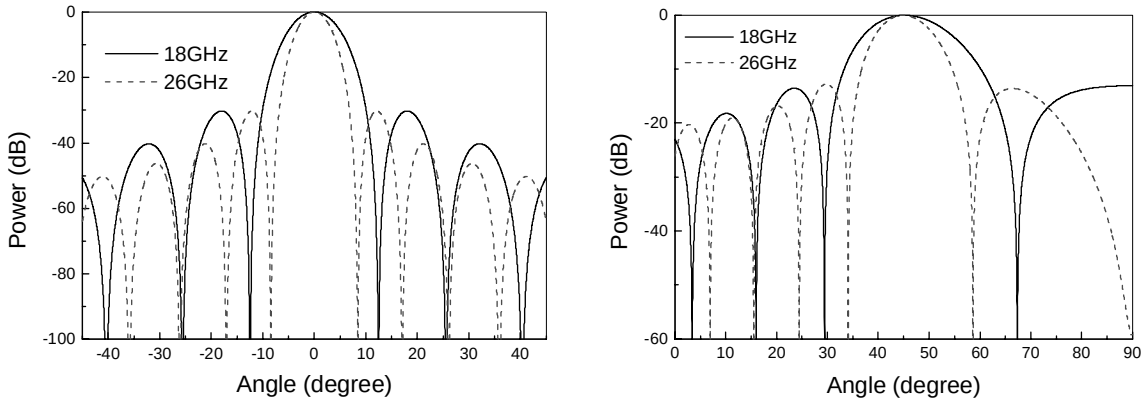

Fig.5. The far-field radiation pattern of PAA at the hybrid control scheme
The beamwidth at normal (left) radiation: 7.38º @ 18GHz and 5.02º @ 26GHz;
The squint error from 18 to 26GHz at 45º steering: 0.22º

5. RELEVANT TECHNIQUE

1. Squint free technique for photonic PAA subarray steering

The squint error in the hybrid steering control comes from displacement of the phase centers of the TTD control row and the phase control row, which happens when you change the RF frequency. Fig. 6 illustrates the mechanism. It shows only the first two rows. The last element in the middle row will also be discarded (as we explain below). The solid lines in the ϕ axis show the phase positions of the TTD control row of the array at a certain steering angle, and the

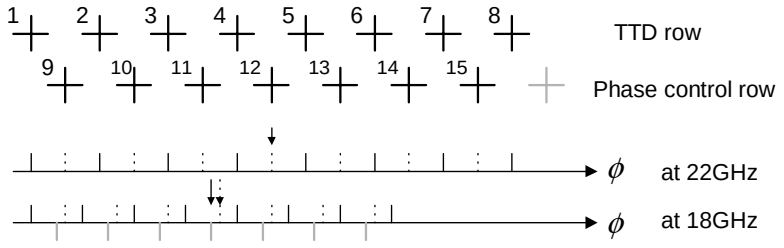

Fig.6 The phase relationship of elements using hybrid steering contol

dash lines show those of the phase control row. Because the phase deviation between {m, m+8} is designed for 22GHz, when the antenna operates at that frequency, it is equal to a complete true-time delay control. But, when the RF frequency changes, 18GHz for example, this phase deviation cannot automatically transform to the desired values (marked by the gray solid line under the ϕ axis) as those do among the TTD controlled elements. As a result, the phase centers (marked by the arrows in the figure) of two rows of elements will have a displacement as shown. This displacement causes the squint because these two rows have the same symmetric center in the real physical space. If we do not discard the 16-th element, the symmetric center of the phase control row would have a displacement with the TTD row in real space, so the displacement between their centers in phase domain is needed. However, we found that, when you add the 16-th element to the phase control row, the resulting phase centers' displacement will be larger than the desired value by exactly the same amount as the one in the case without the 16^{th} element. And because now the radiation of the phase control row has the same amplitude as the TTD row, the squint is even worse.

So, the issue is finding a method to locate the phases of the middle row of the elements at the positions that have been marked by the gray solid line in the figure. We can see that the position of each gray solid line is located at the middle point between neighbored phase positions for TTD controlled elements. So, the desired phase value for the each element in the middle row is the average of the phase values for its neighboring elements in the TTD row. This is easily to by adding the two TTD signals together. Take for example the elements {1, 9, 2}. Fig. 7 shows the adding operation, and another, more universal operation, as well as the corresponding phase vector relatioships.

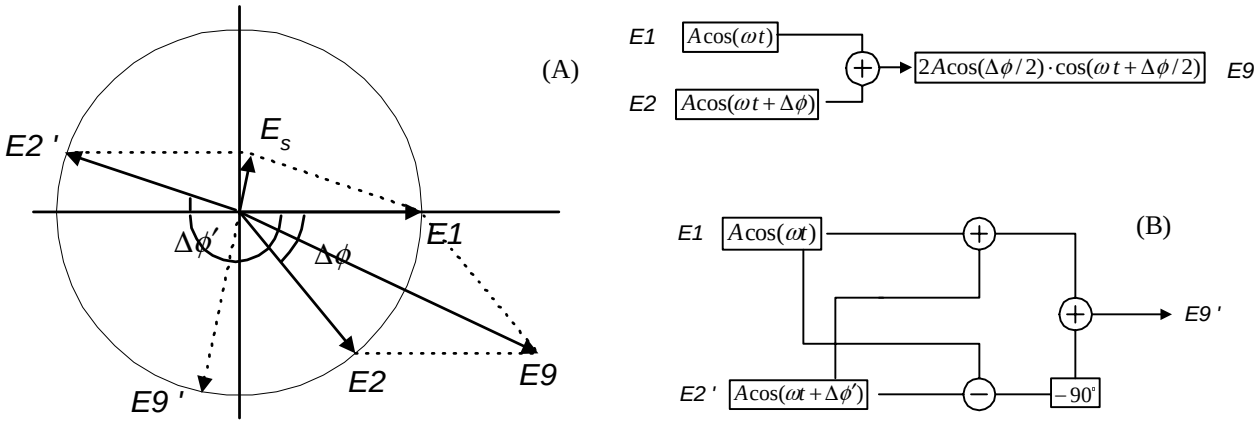

Fig.7. Operation for the steering control of the middle row's elements, (A) simple adding; (B) modified operation

The simple adding operation is appliable only when the phase difference $\Delta\phi$ is smaller than π. As shown in Fig.7, the signals $E1$and $E2$ are the true-time delay control signals to the elements No.1 and No.2, respectively. The phase delay of the sum signal $E9$ is just half of $\Delta\phi$. Of course, before we send it to the No.9 element for radiation, an amplitude adjustment is needed in order to make it equal the others. This can be accomplished by an antomatic-gain-control (AGC) circuit. When the phase difference between $E1$ and $E2$ is larger than π (as happens in our system when the RF frequency is larger than

21.97GHz), the simple adding operation can no longer give the signal with the correct phase. An operation of some complexity will be needed. In the figure, signal $E2'$ has a phase delay $\Delta\phi'$ that is larger than π; the sum signal E_s and the desired signal $E9'$, actually have opposite directions. However, we can not simply reverse E_s and then amply it to get $E9'$, because the resulting operation does not apply when $\Delta\phi$ is smaller than π.

The universal operation is shown in the figure by (B) diagram. The difference vector between $E1$ and $E2'$ always has a 90º phase difference with $E9'$, so the operation $-j(E1-E2')$ should give out the signal with a correct phase delay. However, in some cases, $\Delta\phi$ equals the integer times 2π (for example, at normal radiation or higher RF operation so that ΔX in array lattice has been larger than radiation wavelength). When this difference vector equals zero, the operation cannot be performed. To make the operation universal, we add in the sum signal again after the operation $-j(E1-E2')$, and the final solution for the subarray steering control then becomes the (B) operation in Fig.7. The only shortcoming is that, when $\Delta\phi$ is larger than $3\pi/2$, the opposite vector E_s will have a larger amplitude than the difference vector, and in that case the result of (B) operation will not have a correct phase any more. However this will not happen in our system's frequency range. Even when the higher RF frequency (larger than 26GHz) is wanted, the (B) operation in Fig.7 still can provide the correct steering control up to the point where the frequency is larger than 32.97GHz.

Thus the signals for the other elements in the middle row can be obtained from the same operation applied on their neighboring true-time delay controlled elements. To state this as clearly as possible, the signal for No. k element will come from the signals for No. k-8 and No. k-7. Fig. 8 is the simulation result of the far-field radiation pattern of a 45º steering angle when we use the 8-channels of true-time delay signals to control the first row (No.1 to No.8 elements) and use the (B) operation in Fig.8 to control the middle row (No.9 to No.15 elements). It is found that the squint error disappears as we expected and the beamwidth is smiliar with the typical hybrid scheme. The subarray steering control technique we propose here can reduce the control varables by half the amount, while one can still have the full true-time delay control feature. It will be very helpful for an array antenna with alarge number of elements.

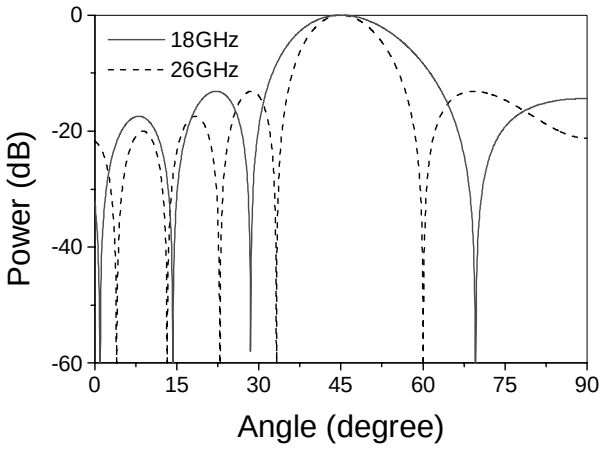

Fig.8 Far-field of radiation pattern at 45º steering angle using squint-free subarray control

2. Heterodyne generated photonic RF source

The principle of heterodyne RF generation can be simply experessed by the following equations,

$$\begin{aligned} I_H(t) &= [E_1(t)+E_2(t)]\cdot[E_1(t)+E_2(t)]^* \\ &= \left|A\exp[-j(\omega_1 t+\varphi_1)]+A\exp[-j(\omega_2 t+\varphi_2)]\right|^2 \\ &= 2A^2+2A^2\cdot\cos[(\omega_1-\omega_2)t+(\varphi_1-\varphi_2)] \end{aligned} \tag{7}$$

where, $E_1(t)$ and $E_2(t)$ are the optical field intensities of the two channels of light, respectively. $I_H(t)$ is combined optical intensity. The last item in the third line is just the RF signal that we need. The RF frequency will be determined by the optical frequency difference ω_1-ω_2. After the photodetector, the resulting RF signal power will be:

$$P_{RF} = \frac{1}{8} Z_L R^2 (P_{opt.p})^2 \tag{8}$$

Here Z_L is the load impedance of detector, R the responsivity of detector, and $P_{opt.p}$ the peak power of the optical signal. According to (7), $P_{opt.p}$ is equal to four times the optical power of each channel. This also reflects the advantage of using a heterodyne to generate an RF photonic signal compared to the direct modulation method. This formula is derived from the ideal case represented by (7), in which the two channels of light have the same polarization and the same amplitude. So, it is the theoretical limit for the conversion effeciency of heterodyne photonic RF system.

Using the heterodyne method, we easily raised the RF frequency up to 100 GHz. The question remaining is how to increase the conversion efficency. The critical issues are to ensure that two optical beams have the same polarization and amplitude, very stable frequencies, and freedom from phase noise as possible as we can. Using two tunable external cavity lasers working at about 790nm, we have succesfully demonstrated a heterodyne system in which conversion effeciency approaches the theoretical limit defined by (8). Its block diagram is shown in Fig.9, as well as the spectrum line of the generated RF signal. Careful alignment allowed both channels to have the same optical power (-12dBm) coupled into the fiber. We monitored this procedure with an optical spectrum analyzer. Both lasers have the same polorization (vertical), and a linewidth of less than 10MHz.

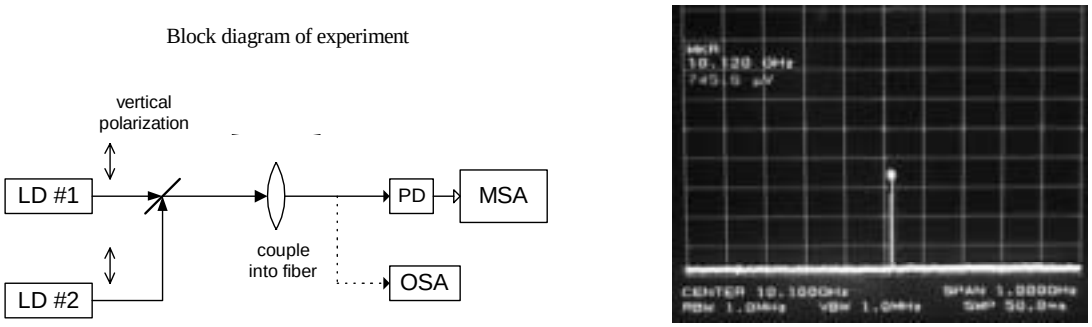

Fig.9 Heterodyne photonic RF signal generation, OSA: optical spectrum analyzer; MSA: microwave spectrum analyzer

The photodetector that we used has the responsibility of 0.18A/W. Based on formula (7), -12dBm channel optical power will produce –48.9 dBm RF power in the ideal case. The measured RF signal power is –49.6dBm in our experiment, as seen in Fig.8. They are quite close.

6. CONCLUSION

We have presented our new substrate-guided wave optical beamforming network for phased-array antenna true-time delay steering. The network is based on the optical Blass matrix realized by our 2-D substrate-guided wave fanout structure. A photonic phased-array antenna system using this optical feeding network has been designed and is under preparation. The whole system will work on 18-26GHz, which will be the photonic PAA demonstration with the highest RF frequency. We have proposed a new squint-free technique for the steering control of photonic phased-array antenna in which the optical true-time delay control is needed only among subarrays. We have reported the simulated result of its far-field radiation pattern without squint error. We have built a heterodyne system for photonic RF signal generation, with a conversion efficiency approaching the theoretical limit.

7. REFERENCES

1. Yoshihiko Konishi, etc., "Carrier-to-Noise Ratio and Sidelobe Level in a Two-Laser Mode Optically Controlled Array Antenna Using Fourier Optics", *IEEE Transactions on Antennas and Propagation*, Vol. 40(12), pp. 1459-1465. 1992.
2. D. Dolfi, etc., "Experimental demonstration of a phased-array antenna optically controlled with phase and time delays," *Applied Optics*, Vol. 35(26), pp. 5293-5300, 1996
3. Dennis T. K. Tong and Ming C. Wu, "A Novel Multiwavelength Optically Controlled Phased Array Antenna with a Programmable Dispersion Matrix," *IEEE photonics Technology Letters*, Vol. 8(6), pp. 812-814, 1996.
4. Akis Goutzoulis, Ken Davies, etc., "Development and field demonstration of a hardware-compressive fiber-optic true-time-delay steering system for phased-array antennas," *Applied Optics*, Vol. 33(35), pp. 8173-8185, 1994.
5. E. Ackerman, etc., "Integrated 6-bit photonic true-time-delay unit for lighweight 3-6 GHz radar beamformer," *IEEE International Microwave Symposium Digest*, Part 2, pp.681-684, 1992.
6. C. T. Sullivan, etc., "Switched time delay elements based on AlGaAs/GaAs optical waveguide technology at 1.32μm for optically controlled phased array antennas," *Optical Technology for Microwave Applications VI and Optoelectronic Signal Processing for Phased-Array Antennas III, Proc. SPIE* Vol. 1703, pp. 264-271, 1992.
7. W. Ng, R. Loo, etc., "Silica-waveguide optical time-shift network for steering a 96-element L-band conformal array," Optical Technology for Microwave Applications VII, A.P. Goutzoulis editor, *Proc. SPIE* Vol. 2560, pp. 140-157 (1995).
8. S. Yehnanarayanan, P. D. Trinh, and B. Jalali, "Recirculating photonic filter: a wavelength-selective time delay for phased-array antennas and wavelength code-division multiple access," *Optics Letters*, Vol. 21(10), pp. 740-742 (1996).
9. Zhenhai Fu, Ray T. Chen, "Compact broadband 5-bit photonic true-time-delay module for phased-array antennas," *Optics Letters*, Vol.23(7), pp. 522-524, 1998.
10. S. Drabowitch, A. Papiernik, H. Griffiths, and J. Encinas, ***Modern Antennas***, Chapman&Hall, pp. 411-414, 1998.
11. Zhenhai Fu, Ray T. Chen, "Waveguide-hologram-based wavelength-multiplexed pseudo-analog true-time delay module for wideband phased array antennas", *Applied Optics*, Vol. 38(14), 1999.
12. Bing Li, Suning Tang, etc., "Switching characteristic of wideband MSM and PIN photodetectors for photonic phased array antenna," in this proceding.